PRIMARY COSMIC RAY PARTICLES WITH Z > 35 (VVH PARTICLES)

G. E. Blanford Jr.,* M. W. Friedlander, M. Hoppe , J. Klarmann,
R. M. Walker and J. P. Wefel**

Laboratory for Space Physics, Washington University
St. Louis, Missouri 63130, U.S.A.

Large areas of nuclear emulsions and plastic detectors were exposed to the primary cosmic radiation during high altitude balloon flights. From the analysis of 141 particle tracks recorded during a total exposure of 1.3 x 10^7 m^2.ster.sec., a charge spectrum of the VVH particles has been derived.

1. Introduction. In a collaboration between the University of Bristol, the General Electric Research and Development Center, the University of California at Berkeley and Washington University, several high altitude balloon flights were undertaken in order to investigate the primary cosmic ray particles with $Z > 30$ (i.e. the VVH particles). After the flights, the packages were divided, with each group analysing its portion independently. The data reported in this paper were obtained from a total exposure of 1.3 x 10^7 m^2.ster.sec., approximately equal to the total exposure of previously published experiments. The most recent review of the observations of VVH particles was given by Price (1971) at the last International Cosmic Ray Conference; the present results together with extensive discussion of experimental details are being published elsewhere (Blanford et al, 1973 a, b).

2. Detectors and Scanning. Four balloon flights provide the observational basis of the present data. All flights were launched from Palestine, Texas and floated over a region where the geomagnetic cutoff averaged around 4.3 GV. Typical flight altitudes were at 3-4 gm/cm^2. The four flights, referred to as Barndoor II and III and Texas III and IV, carried multiple detector layers. All had Ilford G5 emulsions, and a variety of plastic detectors. In order of decreasing sensitivity, these plastics are cellulose nitrate (Daicel); cellulose triacetate (Kodacel and Bayer TN), cellulose acetate butyrate (Bayer BN-CAB) and Lexan (polycarbonate).

Each package also employed a shifter whereby one layer of the detector was moved relative to the rest when the balloon attained float altitude. By matching tracks, we unambiguously identified each event as either ascent of altitude. In Barndoor III, four separate shift positions were used as the balloon drifted in altitude and geomagnetic cutoff during the flight. Only altitude tracks have been included in the further analysis.

*Now at NASA-Johnson Space Center, Houston, Texas, 77058.
**Now at Naval Research Laboratory, Washington, D. C. 20375.

Scanning of the etched plastic sheets was carried out both with the semi-automatic spark scanning technique and with an optical microscope. Layers of Daicel and CTA were etched for long periods in order to produce etched holes that completely penetrated the plastic, and these sheets were then spark scanned. In addition, all tracks found in one layer but not in another (via the spark scanning) were followed in an optical microscope into the other layers to locate incompletely etched tracks. This procedure, of starting with the most sensitive plastic and working through to the least sensitive (lexan) should yield the highest efficiencies. Spark scanning alone for CTA plastic on Barndoor III was found to be 88% efficient, but in combination with optical tracing the efficiency was estimated to be ≥98%.

From the CTA, each track was traced to an etched layer of CAB, and from there to the Lexan. This procedure ensured that each event would be located in the maximum number of layers and it also provides an immediate rough division of the data into broad charge groups, defined by the sensitivities of the plastics, as shown in Fig. 1.

Among the altitude VVH tracks, we have found a group that were due to non-VVH particles with kinetic energies below the geomagnetic threshold. Unless care is taken to identify and exclude these lightly-charged particles, they may be confused with the faster VVH primaries. These observations have been described by Blanford et al, (1972). All results reported in the present paper refer only to fast particles.

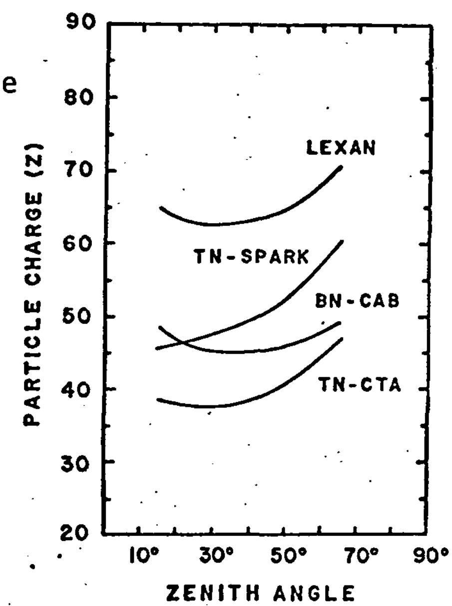

Fig. 1. Charge thresholds for track registration. The two TN-CTA curves refer to spark and optical scanning.

3. <u>Charge Determination</u>. Each of the "fast" VVH events was located in additional layers of plastic that were etched in rigourously controlled conditions, and the track etching rate V_t was computed from measurements on the resulting etched cones. The track etching rate is connected to the charge and energy of the particle via the ionization. With calibration being based upon low energy Fe primaries recorded and also with ions from the HILAC accelerator. This calibration differs from that employed by other workers, and has been discussed by Blanford et al, (1973a), who also treat the assignment of effective kinetic energy. (This is needed for the ionization depends on energy which is not measured but only poorly defined by the cut-off.)

On several flights, events were also measured in nuclear emulsions using a photodensitometer and methods as described by Fowler et al, (1970). In the figure below (Fig. 3a & b) there are shown the results of the comparison of charge assignments based on independent measurements in different detectors.

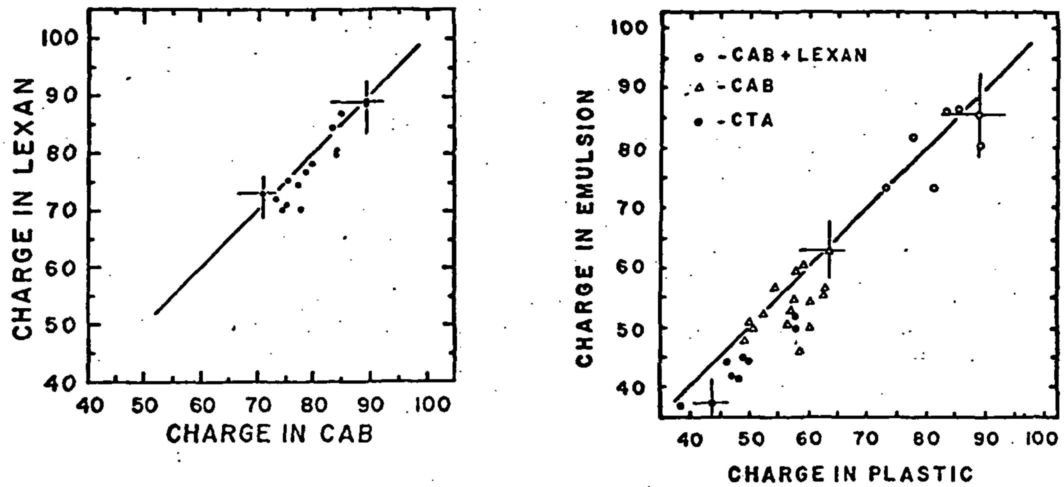

Fig. 3. Comparison between charge assignments in Lexan and CAB plastics, and between emulsion and plastics. Typical error bars are shown for only a few representative points.

The overall statistical accuracy of charge assignments is estimated to be $\Delta Z = {}^{+3}_{-6}\%$.

4. <u>Experimental Results and Discussion</u>. Despite the large detector areas and long exposure times, the statistics are quite limited. In view of this, and the experimental charge resolution, we have divided the charge spectrum into groups each normally 5 charge units wide. The heaviest group is defined as those with $Z \geq 86$; this division was used because, within our charge resolution, it was felt that an apparent charge of 84 or 85 would most probably represent a genuine $Z = 82$ or 83 rather than $Z \geq 90$.

The final charge assignment for each event was the average of all plastic and emulsion measurements, made in the various layers. This was true for all except for $Z \leq 40$ particles for which no plastic charge measurements were available; these events were located via the Daicel scanning, and their charge values rest entirely on emulsion measurements. The lower boundary of the lowest charge group is set by the threshold of the Daicel. This threshold is not well defined, and there appears to be a varying efficiency near threshold. As discussed elsewhere (Blanford et al, 1973a), we consider here only those events with $Z > 35$, where we are confident we have close to 100% detection efficiency. Measurements on these particles are confined to Barndoor III, while for particles with $Z \geq 50$ all flights were used. The observed spectrum, at detector flight level, is given in Table I.

Above $Z = 50$, the agreement with earlier work is generally good. For charges between 40 and 50, we find a greater flux than do Fowler et al, (1970). It must be emphasised that the

Table I
Charge Spectrum at Flight Level

Charge Group	≤35	36-40	41-45	46-50	51-55	56-60	61-65	66-70	71-75	76-80	81-85	≥86
Events	20	19	22	13	21	22	10	3	10	8	5	3
Flux x 10^6 /m^2.ster.s.	10±2	10±2	11±2	6±2	2.0±0.5	1.7±0.5	1.0±0.3	0.4±0.2	0.9±0.3	0.9±0.3	0.5±0.2	0.2±0.2

the data in the Table represent combined data from four flights, in which there were different area-solid angle factors for the different charge groups.

To determine the flux of each group of particles, the flight-level spectrum for each flight (i.e. the component data of Table I) was extrapolated to the top of the atmosphere and only then was the total spectrum obtained. Because of uncertainties in the fragmentation parameters for VVH-particle collisions in the atmosphere, we prefer to quote flux values in broader charge groups, and these are listed in Table II, along with the ratios of observed and solar system abundances to the $20 \le Z \le 30$ group.

TABLE II

FLUX OF VVH PARTICLES AT TOP OF THE ATMOSPHERES

Charge Group	Number of Tracks Used for Flux Computation	Flux[1] (m^2-ster-sec)$^{-1}$ (x 10^6)	Ratio[2] of Flux to that of Fe-group (x 10^6)	Ratio of Solar System Abundances (Cameron) (x 10^6)
35 - 40	19	16 ± 4	33 ± 8	176
41 - 50	35	28 ± 6	57 ± 12	14
51 - 60	47	7 ± 1	14 ± 2	22
61 - 70	13	2.3 ± 0.6	4.7 ± 1.2	2
71 - 85	24	3.5 ± 0.7	7.1 ± 1.4	7
≥ 86	3	0.8 ± 0.5	1.6 ± 0.9	—

Notes: 1. Geomagnetic cutoff specifies the minimum rigidity; the corresponding cut-off kinetic energy thus varies with (Z/A). Flux values have therefore been normalized to a standard kinetic energy of 1.0 GeV/nucleon, the cut-off value for the highest charge group. An integral energy spectrum with slope -1.5 has been assumed for this normalization.

2. The flux of the Fe-group is usually quoted at 0.4 particles/m^2-ster-sec. This is appropriate for the usual cut-off rigidity over Texas; for computing the ratio of the VVH particle fluxes to the Fe-group, the Fe-group has also been normalized (as above) to a kinetic energy of 1.0 GeV/nucleon, leading to a flux of 0.49 particles/m^2-ster-sec.

The apparently low abundance of the 36-40 group cannot be due to the choice of the lower boundary for this group. We find (and have listed in Table I) only 20 particles with measured charges $Z \le 35$, and even if a large proportion of these should properly have been classed with the (36-40) group, there would still remain a significant discrepancy. Contamination of the (41-50) group by unrecognised slow (but lighter) particles is considered unlikely, as many have already been removed in the earlier analysis.

5. Conclusions. We have found three events with $Z > 86$, with actual assigned values of $Z = 90$, or, within the experimental uncertainties, possibly $Z = 92$. No transuranic nuclei were found. Because of charge resolution limitations it is difficult to separate $Z = 93$ or 94 from $Z = 90$-92, but the observation of trans-bismuth particles provides evidence, yet again, that r-process nucleosynthesis must be involved in the source of VVH cosmic rays.

The significant underabundance of the (36-40) group reported here might seem to suggest that the r-process dominates throughout the spectrum, since the production of the (36-40) group via the r-process is much less (about 1/3) than in the s-process. However, both r and s processes contribute about equally in the (41-50) group, and the presumption of r-process dominance cannot explain the observed overabundance in this (41-50) group.

We thus find that the details of the charge spectrum, even with the modest charge resolution and statistics so far attained, cannot be fully explained by one nucleosynthesis process, and more detailed models are required. Paper 163 at this meeting (Blanford et al.) is addressed to a more detailed examination of the implications of the charge spectrum observed for $Z > 50$.

6. Acknowledgements. We are grateful to our colleagues for their help at the earlier stages of our collaboration, and to the flight crews at the N.C.A.R. Balloon Facility in Palestine, Texas, for their unfailing competence. Thanks are also due to our scanners for all of their work. This research has been supported under N.A.S.A. Grant NGR-26-008-1 and N.S.F. Science Development Grant GU-1147.

References

BLANFORD, G. E. Jr., M. W. Friedlander, J. Klarmann, S. S. Pomeroy, R. M. Walker and J. P. Wefel, (1972), J. Geophys. Res. 77, 6037.

BLANFORD, G. E. Jr., M. W. Friedlander, J. Klarmann, S. S. Pomeroy, R. M. Walker, J. P. Wefel, P. H. Fowler, J. M. Kidd, E. J. Kobetich, R. T. Moses and R. T. Thorne (1973a), Phys. Rev. (in course of publications).

BLANFORD, G. E. Jr., M. W. Friedlander, J. Klarmann, R. M. Walker and J. P. Wefel (1973b), Phys. Rev. (in the course of publication).

FOWLER, P. H., V. M. Clapham, V. G. Cowan, J. M. Kidd and R. T. Moses, (1970), Proc. Roy. Soc. London A318, 1.

PRICE, P. B., (1971), Rapporteur Paper, 12th International Conference on Cosmic Rays, Hobart, Tasmania.